Slovak Geol. Mag., 8, 3– 4(2002), 235 – 246

Shear deformation in granodiorite: Structural, $^{40}Ar/^{39}Ar$, and geotechnical data (Tribeč Mts., Western Carpathians)

JÁN KRÁĽ[1], JOZEF HÓK[1], WOLFGANG FRANK[2], PAVOL SIMAN[1], PAVEL LIŠČÁK[1] & VLASTA JÁNOVÁ[3]

[1]Geological Survey of the Slovak Republic, Mlynská dolina 1, 817 04 Bratislava, Slovakia
[2]Geozentrum, Universität Wien, Althanstrasse 14, A - 1090 Wien, Austria
[3]Ministry of the Environment of the Slovak Republic, nám. Ľ. Štúra 1, 812 35 Bratislava, Slovakia

Abstract. A shear zone in granodiorite has been studied in the Tribeč Mts. Whole rocks and mineral samples from deformed and undeformed rock types have been processed by means of structural, geotechnical and $^{40}Ar/^{39}Ar$ methods. The shear zone was formed by progressive simple shear in ductile to brittle-ductile conditions. The quartz isotropic microfabrics of the undeformed host rocks have been progressively transformed into anisotropic microfabrics composed of single oblique girdle indicating sinistral shear. A simple shear deformation was responsible for the formation of "s" and "c" foliations. Shear strain has been calculated for particular parts of the shear zone. Geotechnical data show the decrease of mechanical index parameters of rocks towards the centre of the shear zone. Decreasing of SiO_2, MgO and Na_2O content and increasing of Al_2O_3, CaO, K_2O and Fe_2O_3 in the same direction have been documented. $^{40}Ar/^{39}Ar$ data of white micas from centre of the shear zone proved its formation about 71–63 Ma ago. Obtained ages are interpreted as shear zone formation age . $^{40}Ar/^{39}Ar$ biotite apparent age spectra from undeformed granodiorite samples reveal significant Ar excess.

Key words: granodiorite, shear zone, structural data, $^{40}Ar/^{39}Ar$ dating, mechanical properties, Tribeč Mts., Western Carpathians

Introduction

Geological mapping (Ivanička et al., 1998) revealed in the Zobor part of the Tribeč Mts. (sensu Vass et al., 1988) a tectonic zone of NE-SW trend, being accompanied with intensive mylonitization of granitoid rocks. The length of the zone is app. 10 km, the width varies from several hundreds to several tens of metres. The rock deformation inside the zone is not homogeneous. A segment of this tectonic zone is exposed in the northwestern - Zobor part of the Tribeč Mts. in termination of the Malé Jastrabie Valley (Fig. 1). The mylonitic zone with transitions from deformed granitoid rocks towards undeformed ones is exposed there in the outcrop of app. dimensions 5 m x 5 m x 3 m. Mylonitic zone, resp. shear zone of the brittle-plastic character, is developed in the medium-grained biotitic granodiorites to tonalites (Ivanička et al., 1998). Broska & Petrík (1993), Petrík et al., (1994) ranked these types of granitoid rocks to allanite, resp. I-type of granitoid rocks of the Western Carpathians. In the outcrop we have distinguished three domains in relation to the intensity of rock strain from undeformed to the most intensive deformed rocks. The topic of our study included the change of rock properties in individual distinguished domains. We have observed the type and spatial arrangement of tectonic foliation and lineation as well as the change of arrangement of quartz optical axes. Isotopic research was focused prevailingly on $^{40}Ar/^{39}Ar$ micas dating from deformed and undeformed types of granitoid rocks. The last observed topic covered the geomechanic properties of rocks and their changes in relation of tectonic rock strain.

Methodics

Using macroscopic criteria for the evaluation of the deformation degree we have distinguish three domains in studied locality/outcrop. These differ each another prevailingly by the different intensity of tectonic foliation development (Fig. 3). The first domain is without any presence of visually recognizable tectonic overprint. The second one is characteristic with the presence of "s-planes" of tectonic foliation. Third domain manifests strong development of "c-planes" of tectonic foliation, next the intensive macroscopically observable deformation of minerals and development of definable stretching lineation.

Structural analysis consisted from identification and determination of spatial characteristics of principal structural elements (foliation, mineral lineation). Structural data were graphically analysed using tectonograms (e.g. Fig. 3). Oriented thin-sections allowed to observe the microstructures. Orientation of optical quartz c-axes was defined using standard methodics by universal stage (c.f. for instance Fediuk, 1961).

Slovak Geol. Mag., 8, 3– 4(2002), 235 – 246

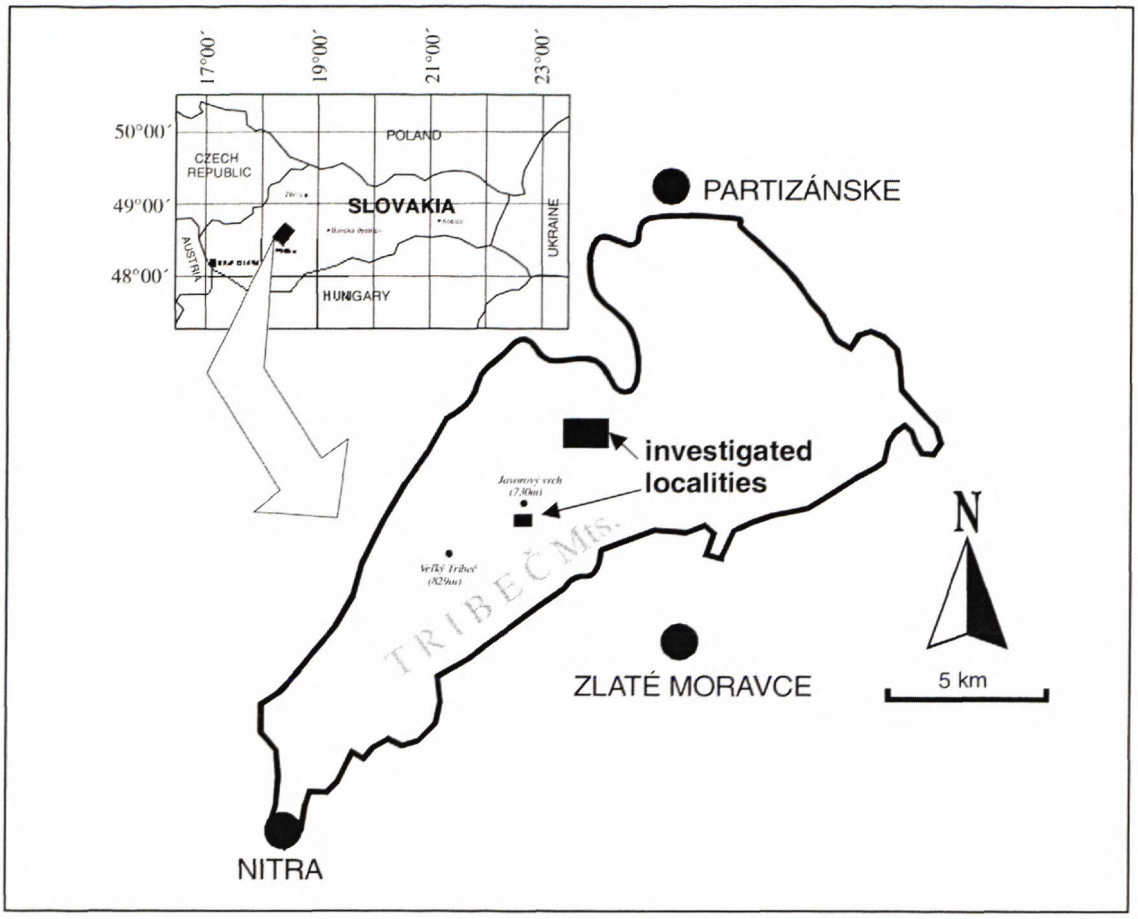

Fig. 1 Position of investigated localities in the Tribeč Mts.

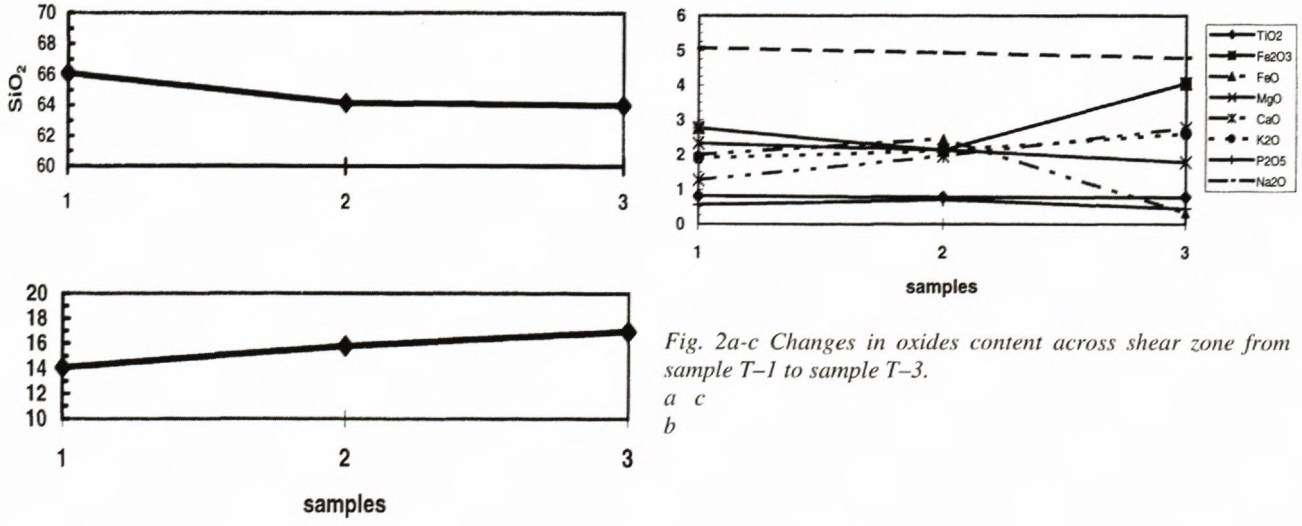

Fig. 2a-c Changes in oxides content across shear zone from sample T–1 to sample T–3.
a c
b

The index mechanical characteristics of rock massif/material were tested by the Schmidt's rebound hammer as well as the Point Load Test (PLT). To learn the resistance of rock against weathering we used the Slake Durability Test.

Schmidt's rebound hammer for simply and quick testing of rock rebound hardness allows to obtain an information on a broad physical state of rocks in the massif. Simultaneously it allows to distinguish in measured profile the horizons with differing degree of rock weathering (resp. other alterations). It is useful for qualified estimation of rock strength characteristics.

Point Load Test - PLT - $Is_{(50)}$ [MPa] allows prompt determination of rock strength. Test consists from registration of rock resistance against the imposed stress through two co-axially arranged conic platen points. The examination can be carried out on regularly shaped (square, cylindrical roller) or irregular (fragments) samples.

Slake Durability Test was used for evaluation of "rock durability". From each rock we prepared 20 fragments weighting app. 50 g (using 10 fragments into two rotating drums). Fragments were thoroughly washed and easily removable roughnesses and edges were retrieved. Consequently they were dried using temperature 105 ^{0}C till their steady weight. We placed two samples of the same rock type into the perforated steel drums with holes of 2 mm diameter. Both drums were fixed to apparatus in such a way to be submerged into the water container to the water level reaching the level approximately 2 cm beneath the drum rotation axis. The drums` rotation by velocity 20 turns per minute lasted two minutes. Afterwards the samples were taken off the drum and dried in drying-oven to steady weight. The whole cycle was repeated 3-times.

The micas for $^{40}Ar/^{39}Ar$ dating were separated from crushed and sieved rock using the wet shaking table and electrostatic separator. Purification was done using hand separation under binocular magnifying lens and ultrasound in distilled water. Next step was the irradiation by fast electrons together with internal laboratory standard WAP. The isotopic ratios ^{40}Ar, ^{39}Ar were measured from individual gas portions (purified in vacuum quartz equipment by gettering) in increasing temperature, applying the gas mass spectrometer VG-5400. This standard procedure, used in geochronologic laboratory Geozentrum Wien, has recently the individual analytical steps automatized. For age calculations there were used the decay constants by Steiger & Jäger (1977).

Results and disscusion

Description of investigated samples

The primary rock is represented by massive, medium-grained, equigranular light-grey granodiorite to tonalite of I-type, rich in biotite, titanite, allanite and epidote. There are typical the greenish plagioclases with basic cores, as well as bluish grains of quartz reaching dimensions 3-6 mm. The increasing deformation changed the rock character from massive to schistose with expressive foliation and often with abundant sericite, occasionally only with Fe oxides and hydroxides in foliation planes. This rock has greenish to grey-green colour with the white deformed feldspar porphyroclasts. Green character is caused by the presence of newly-formed phyllosilicate sericite and chlorite phases, eventually chloritized biotite.

The undeformed granitoid rocks have hypidiomorphic crystal shape, with modally the equal presence of quartz and plagioclase grains reaching dimensions up to 6 mm. Quartz forms the well-preserved hypidiomorphic grains with weak undulose extinction. The plagioclase is strongly sericitized to saussuritized and albitized preferably in its cores with higher basicity, around which albitic rim is developed. Biotite is abundantly present in the form of rests and aggregates being often disintegrated, recrystallized, smaller, but often even of idiomorphic shapes. It has rich green pleochroism in sections X,Y and X,Z, that could indicate the increased content of Fe-component - annite. K-feldspar, if present, forms several mm large strongly perthitized grains. Titanite has form of clearly spinning, broken crystal forms recrystallized to ilmenite. Next minerals, chlorite, rutile, magnesite, zircon and allanite are present accessorially.

Increasing degree of rock deformation markedly reduces the grain-size, mainly in quartz even below 0.1 mm. Quartz occurs in the form of bands (ribbons) with undulose extinction and even in the foamy structure. It behaves considerably plastically. It is possible to observe the grain boundaries migration. Contrary to this, the feldspars affected by the same changes, sericitization to saussuritization, eventually by perthitization, demonstrate more rigid behaviour with gaining of preferred orientation. Biotite is changed to chlorite and this one together with sericite, as the main weakened minerals became the main bearer of deformation. The rock structure gradually changes from porphyroblastic to mylonitic with clear preferred orientation and lineated phyllosilicates. In the last stage of deformation the rock became totally disintegrated, schistose and oriented. Quartz has very fine-grained polygonal structure with steeply decreasing grain-size below 0.1 mm. Feldspars and biotite are totally disintegrated into chlorite-sericite mass. Biotite is not present since. Its existence is confirmed only by the presence of chlorite with ilmenite clusters.

Described deformation is possible to consider as relatively low-temperature alteration within greenschists facies. It results from the phase change of biotite to chlorite where Eggleton & Banfield (1985 in Shelley, 1993) suppose for the chloritization the temperature 340 °C. In this case the more interesting is the strongly plastic behaviour of quartz during the rigid behaviour of feldspars. The very high strain rate could be supposed in this case.

To complete the presented data we introduce also the results of the chemical analyses of selected oxides from samples taken transversally through the mylonite zone from undeformed granodiorite (sample T-1), protomylonite (sample T-2) and mylonite (sample T-3; Fig. 2a, b, c). The graphs demonstrate the decrease of SiO_2, MgO and Na_2O content towards the centre of mylonitic zone. On the contrary, the content of Al_2O_3, CaO, Fe_2O_3 and K_2O increases.

Structural geology

From the viewpoints of tectonodeformation processes the rocks in the outcrop scale can be alternatively divided into three groups (Fig. 3): undeformed granitoids without macroscopically and microscopically visible deformation structures, medium deformed granitoids being according to the classification by Sibson (1977, 1980) denoted as protomylonites and intensively deformed granitoid rocks - mylonites (sensu l.c.).

Undeformed granitoids (Fig. 4) macroscopically do not express any tectonic overprint with exception of

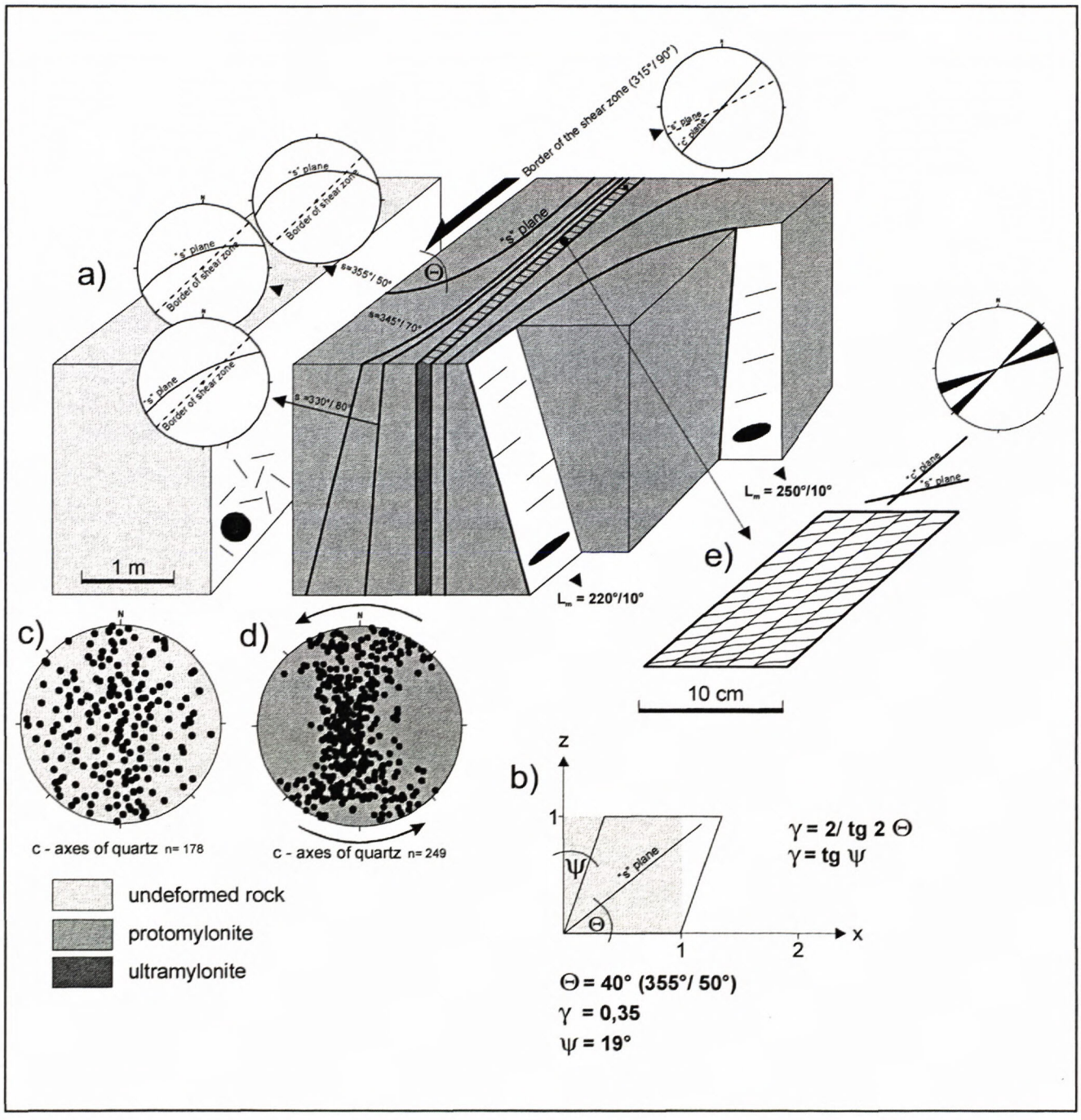

Fig. 3 Simplified sketch of the shear zone a) simplified sketch with observed structural elements, intensity of shading corresponds to intensity of deformation, arrow indicates sense of movement, diagrams display orientation of the "s" and "c" planes and shear zone border: 315°/ 90° (Lambert projection, lower hemisphere), Θ angle between "s" plane and shear zone border, L_m stretching lineation ; b) method of calculation and graphic demonstration of the homogeneous simple shear deformation of the unit square / circle, Θ angle between "s" plane and shear zone border, Ψ - shear angle, γ - shear strain; c) fabric of quartz diagram from undeformed granodiorite ; d) fabric of quartz diagram from protomylonite (n - number of measurements); e) simplified sketch of central part of the shear zone with rose diagram of orientation "s" and "c" planes

joints, being oriented in two general perpendicular directions NW-SE and NE-SW. The orientation of optical quartz c-axes is isotropic and has no more impressive preferred orientation (Fig. 3c).

The qualitatively new planes of planar anisotropy described as schistosity or s-planes (Figs. 5 and 6) originate in deformation domain of protomylonites. These planes are parallel to the plane XY of deformation ellipsoid and originate perpendicularly to direction of the highest pressure. In the ideal case the first s-planes would appear in the rock under the angle 45° to the boundary of shear zone. In observed zone the macroscopically defined s-planes include the angle 40° towards the shear zone. Towards the centre of shear zone the schistosity planes

gradually change their direction and inclination (Fig. 3a). Using the orientation of s-planes it is possible to calculate the shear deformation/strain γ in the rock:

$$\gamma = 2 / tg\ 2\Theta \text{ (c.f. Ramsay, 1980)}$$
$$\gamma = tg\ \psi$$

where Θ represents the angle between the schistosity plane and the boundary of shear zones (Fig. 3b). ψ is the shear angle between the unit deformed object (square, circle) with the "z" axis of the coordinate system (Fig. 3b). On the basis of measured values it is possible to calculate the increment of the shear deformation, the shear angle (Tab. 1) and to express the deformation (Figs. 3b and 7).

Tab. 1: Relationship between the shear strain and orientation of the s–plane.

angle between s–plane and shear zone border	shear strain	shear angle
Θ = 40°	γ = 0,35	ψ = 19°
Θ = 30°	γ = 1,15	ψ = 49°
Θ = 20°	γ = 2,38	ψ = 67°

The results of microstructural study of orientation of optical quartz c-axes demonstrate the anisotropic distribution with the origin of striking belt girdle maximum indicating the sinistral simple shear (e.g. Lister & Williams, 1979). In deformation domain of mylonites being directly in the centre of shear zone we have not succeeded to measure the representative number of quartz optical c-axes, because the quartz grains were tectonically broken into the submicroscopic aggregates.

The centre of shear zone is ca 20 cm wide and the inhomogeneity planes depicted like "c" planes (sensu Berthé et al., 1979) appear there. The "c" planes represent foliations with concentrated shear deformation. The angle between "c" and "s" planes is ca 20° (Figs. 3e and 6). In the case investigated the failure of the rock coherence occurs along the "c" planes and the rock is sheared in brittle regime. This is the reason why the mutual offset of rock blocks in the centre of shear zone is not possible to define precisely.

Physical-mechanical properties

Modified final value of the strength index by the Point Load Test is correlated with the strength in the uni-axial pressure σ_c. The mostly used conversion relation is:

$$\sigma_c = 24 \,.\, Is_{(50)} \text{ [MPa]}$$

Bieniawski (1973) for evaluation of strength suggests to use the classification scale, presented in Tab. 2.

Tab. 2: Estimation of a compressive strength of rocks according Point Load Test (Bieniawski, 1973)

Strength degree	PLT index $Is_{(50)}$ [MPa]	Compressive strength σ_c [MPa]
1.Very high	> 8	> 200
2. High	4 to 8	100 to 200
3. Medium	2 to4	50 to 100
4. Low	1 to 2	25 to 50
5. Very low	< 1	< 25

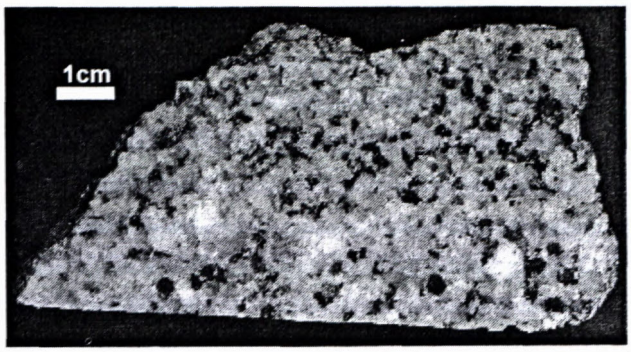

Fig. 4 Photograph of the undeformed granodiorite. Malé Jastrabie locality.

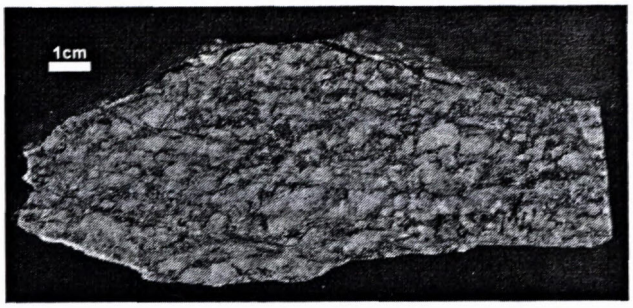

Fig. 5 Photograph of the protomylonite. Note the development of the "s" planes foliation. Malé Jastrabie locality.

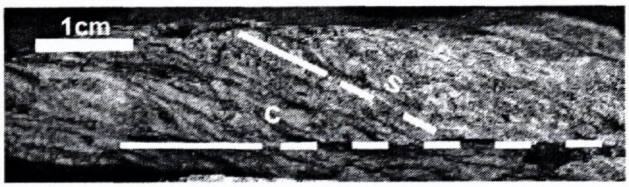

Fig. 6 Photograph of the mylonite. The "s" planes foliation is predominant structure and "c" planes are present as a new structural element. Malé Jastrabie locality.

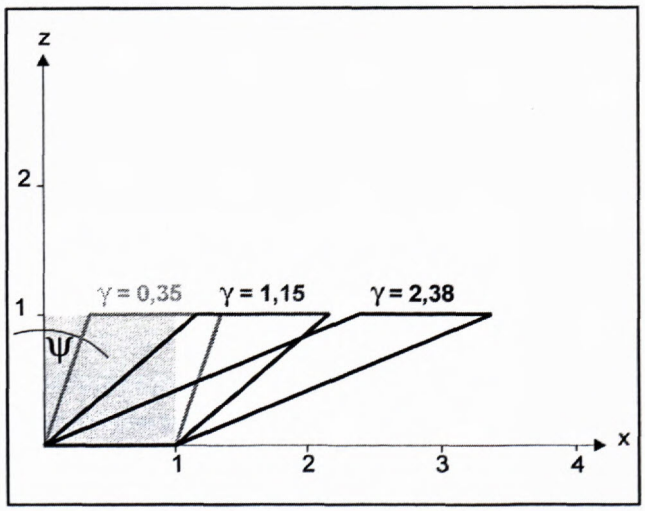

Fig. 7 Graphic plot of data from the Tab. 1, showing progressive shear strain towards the centre of the shear zone.

Slovak Geol. Mag., 8, 3– 4(2002), 235 – 246

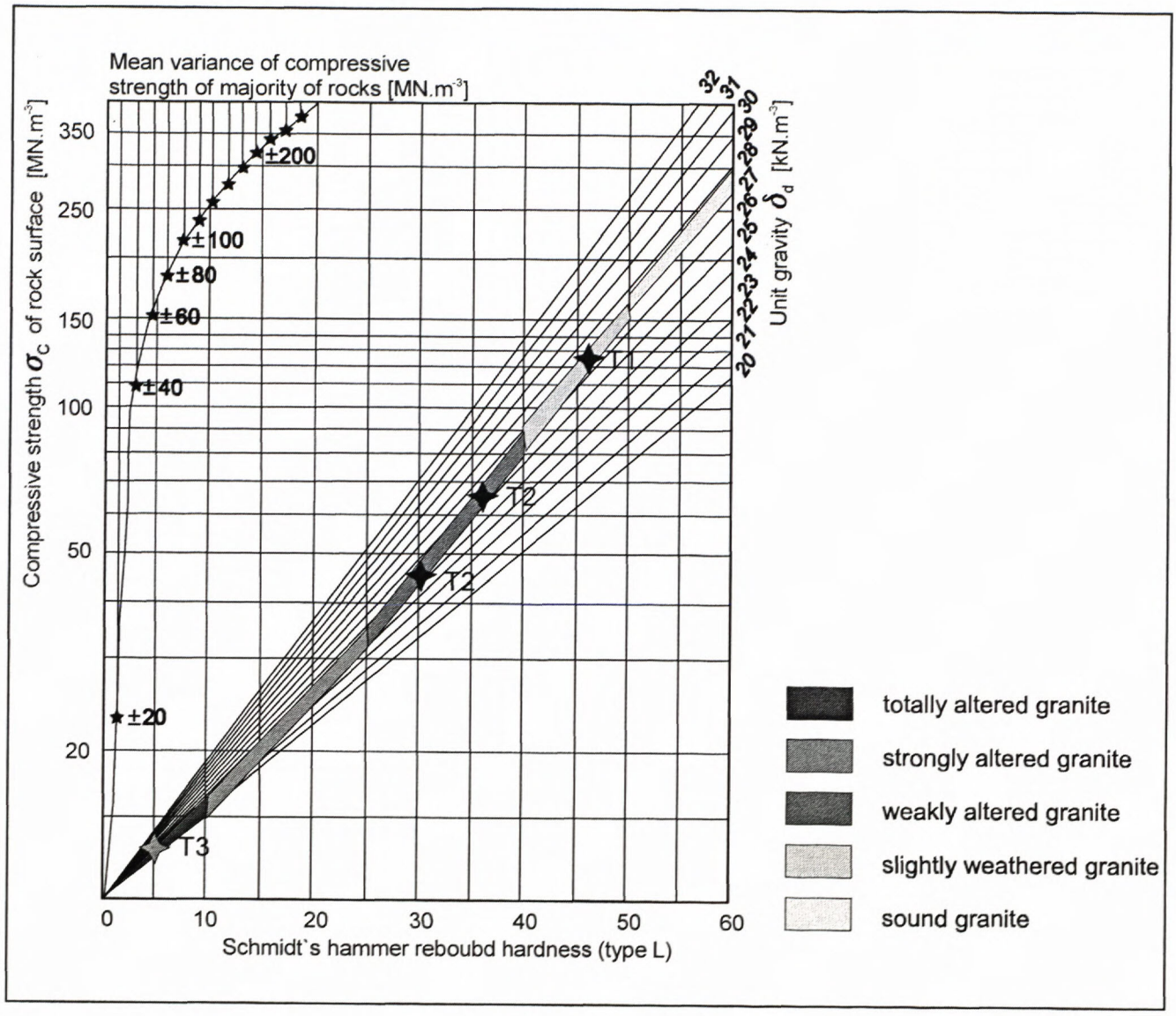

Fig. 8 Evaluation of granodiorite alteration inferred from the Schmidt's rebound hardness.

The results of measurements of rebound hardness are described in graph (Fig. 8). The measuring sample point T-3 was situated in outcrop with the strongest mylonitization. The massif weathering is here the strongest in comparison to the whole outcrop, and is manifested by decrease of strength in uni-axial pressure (value 45.67 MPa ranked the mylonite among the semisolid rocks according to STN 73 1001 Norm). From the centre of mylonitic zone (measurements in sample T-2) the strength in uni-axial pressure increases mainly due to the weakest rock deformation and smaller rock weathering. It confirms the zonality of physical-mechanical properties in mylonitic zone. The sample T-1 represents the weathered granodiorite without evident tectonic failure and it has the highest compressive strength values. The Fig. 8 confirms that derived strength in uni-axial pressure of investigated rock from the centre of mylonite zone is of low-order in comparison with the samples from its periphery.

Very similar values of uni-axial strength in pressure are shown also by the PLT test. It confirms the suitability of the use of both methods for relatively quick and simply determination of this parameter either from technological or geotechnical viewpoints. The indicator of the rock resistance against slaking (slake durability index) is then the percentage ratio of lowered sample weight compared with its original weight.

$$\text{Slake durability index } (I_d) = \frac{\text{original weight - weight after n cycles}}{\text{original weight}} \cdot 100(\%)$$

The examination allows to classify rocks into the six groups:

a/ I_d = 95 - 100 % - rocks with extreme durability,
b/ I_d = 90 - 95 % - rocks with very high durability,
c/ I_d = 75 - 90 % - rocks with high durability,
d/ I_d = 50 - 75 % - rocks with medium durability,
e/ I_d = 25 - 50 % - rocks with low durability,
f/ I_d = 0 - 25 % - rocks with very low durability.

For comparison we list the durability of granitoid rocks also from other localities in the Tribeč Mts. (Tab. 3). In the

Tab. 3: Durability of selected granitoids from the Tribeč Mts. according to Slake Durability Test

Number of sample	Locality	Rock type	Slake durability 1. cycle (%)	Slake durability 2. cycle (%)	Classification according slaking
1	Skýcov	Leucocrate granite	99.50	99.10	Extremely high
2	Skýcov	Slightly weathered leucocrate granite	99.68	99.20	Extremely high
3	Javorový vrch	Granodiorite tonalite, coarse-grained	93.59	93.30	Very high
4	Javorový vrch	Aplitic granodiorite	97.99	97.71	Extremely high
5	Malé Jastrabie	Mylonitized granite	97.89	97.24	Extremely high
6	Malé Jastrabie	Mylonitized granite	97.68	97.10	Extremely high
7	Medvedí vrch	Leucocrate granite	99.70		Extremely high

sense of above stated classification the obtained values of slate durability indicate the durability and resistance of granitoid rocks from the Tribeč Mts. against weathering.

^{40}Ar / ^{39}Ar data

Until recent only the geochronological data from granitoid rocks were published from the crystalline basement of the Tribeč Mts.. The first age from the zircon being separated from tonalite near Janova Ves was published by Bojko et al. (1974). The U, Th/Pb model ages are concordant and vary around 290 Ma. Broska et al. (1990) refined this data from zircons of similar rock for 306 ± 10 Ma. Data can be interpreted as the intrusive age of plutonic rocks (tonalites-granodiorites) in the Tribeč Mts. Rb/Sr datings of the whole rock granodiorite samples are discordant in comparison with these data and older - the slope of published isochron corresponds to the age 352 ± 5 Ma (Bagdasaryan et al.1990). Kováč et al. (1994) published the FT age 28 ± 3 Ma on accessory apatite from tonalite.

The analysed mineral samples were separated from three sample types - undeformed granodiorite - (T-1), from partly deformed granodiorite (T-2, T-7) and from the centre of mylonite zone (T-3). Samples T-1, T-2 and T-3 were taken from the distance ca 20 m from the area of distinct mylonite zone developed in granodiorite.

The principal analytic data together with plots of apparent $^{40}Ar^*/^{39}Ar$ ages (decay constants according to Steiger a Jäger, 1977) are given in Tabs. 4-10 and Figs. 9 - 15.

The biotite was separated and analysed from the samples of undeformed granodiorites T-1, T-8, T-9. $^{40}Ar/^{39}Ar$ spectra are discordant and all apparent ages of individual temperature steps are markedly higher as U-Pb data from zircons of petrographically identical rocks, limiting the intrusion age for 306 Ma (Fig. 9, 14, 15).

The only separable mineral suitable for dating of deformed granodiorite T-2 was the fine light-coloured mica because the former biotite was strongly chloritized. More than 60 % of ^{39}Ar from the sample was degassed in four last high-temperature steps (Fig. 10). This part of the spectrum gives the corresponding plateau age 155 ± 9 Ma.

From the sample T-3, representing the typical mylonite, we have separated and analysed two minerals - fine white mica (sericite) and coarse-grained muscovite. The $^{40}Ar^*/^{39}Ar$ spectrum of apparent ages in sericite has continual staircase shape, where for the higher degassing temperature the apparent age is ca 73 Ma, and in the lowermost degassing temperature the age is 63 Ma. Apparent $^{40}Ar^*/^{39}Ar$ ages of muscovite from the same sample (Fig. 12) have discordant character, mainly in the higher temperature part of the spectrum. The degassing of muscovite is represented by plateau age 72 ± 2 Ma, that is in the range of analytical error corresponding with the higher age from fine-grained light-coloured mica, separated from the same sample.

Biotite from deformed granodiorite T-7 has slightly concave shape, steeper in the high-temperature part of the spectrum (Fig. 13). Lowermost apparent ages in the middle part of the spectrum are forming three medium-temperature steps with data 81-82 Ma.

Though micas are widely used in K/Ar geochronology, in metamorphic terranes the obtained data are most frequently interpreted like the age of cooling, because their blocking temperatures are lower than the ages of many metamorphic, resp. plutonic processes. Therefore they are used rather for the reconstruction of temperature history of investigated area than for the identification of ages of plutonic, resp. metamorphic processes. Despite the usually well readable and interpretable spectra of e.g. phengite, the biotites manifest various types of spectra, which interpretation might be complicated. One of the reasons is the presence of the excess argon. In such cases the apparent age spectra can be smoothed in all temperature steps and the shallow-brained analyses of the data can lead to the age significant spectra of minerals untouched by temperature. Spectra obtained from biotites, resp. minerals with excess Ar might be also of convex or concave shapes (the relevant literature to this problem is discussed by McDougall & Harrison, 1988). The interpretation of such spectra is therefore necessary to be supported also by another geochronologic information in context of relating knowledge from regional geology.

From the comparison of blocking temperatures of U/Pb system in zircons and K/Ar system in micas there follows, that K/Ar ages of biotite in plutonic resp. meta-

morphic rocks will be lower than the real age of plutonic, resp. high-temperature processes. It was confirmed also by a big amount of published data from various geological areas. The magnitude of the difference in obtained U/Pb and K/Ar ages in the case of the simplest thermic history – monotonous cooling - depends on cooling rate. The comparison of data from the Western Carpathians – preferably from core Mountains, where the idea of monotonous cooling during uplift in Hercynian evolution can be accepted - confirms this model (the Malé Karpaty Mts. - Bagdasaryan et al. 1977, Shcherbak et al. 1988; the Malá Fatra, Mts. – Shcherbak et al. 1990, Hók et al. 2000; the Veľká Fatra Mts. – Kohút et al. 1998; the Strážovské vrchy Mts. – Kráľ et al. 1997; review of available K- Ar data and their new interpretation from the crystalline basement of the Western Carpathians till 1985 is available in Burchart et al. 1987), though records about Alpine influence in these rocks were documented by Maluski et al. (1993).

Tab. 4: $^{40}Ar/^{39}Ar$ analytical data from biotite, undeformed granodiorite T-1, Tribeč Mts.

Step	T(C°)	% $^{39}Ar^*$	% $^{40}Ar^*$	$^{40}Ar/^{39}Ar$±2s. d.(%)	Age (Ma) ± 2s.d.
1	620	21.5	95.5	44.83 ± 0.3	348.5 ± 1.1
2	690	11.5	97.2	45.34 ± 0.6	352.1 ± 1.9
3	830	7.0	97.1	45.34 ± 0.4	352.1 ± 1.2
4	1060	45.4	97.2	45.49 ± 0.2	356.4 ± 0.7
5	1350	14.6	97.9	46.49 ± 0.3	360.3 ± 0.9

J = 0.004530 ± 0.4 % total gas age: 354.5 ± 2.8

Tab. 5: $^{40}Ar/^{39}Ar$ analytical data from fine-grained white mica, deformed granodiorite T-2 (protomylonite), Tribeč Mts.

Step	T(C°)	% $^{39}Ar^*$	% $^{40}Ar^*$	$^{40}Ar/^{39}Ar$±2s. d.(%)	Age (Ma) ± 2s.d.
1	585	11.3	54.2	13.72 ± 11.0	113.6 ± 12.2
2	605	3.9	47.0	21.46 ± 30.7	174.9 ± 51.3
3	635	5.8	55.7	18.88 ± 18.3	154.7 ± 27.1
4	670	7.1	58.9	15.37 ± 14.7	126.8 ± 18.0
5	710	7.2	67.5	16.39 ± 13.4	135.0 ±17.4
6	750	7.2	58.2	18.78 ± 2.2	153.9 ± 3.2
7	790	9.9	59.5	18.68 ± 3.1	152.6 ± 4.5
8	830	5.9	68.4	17.10 ± 6,5	140.6 ± 8.9
9	1220	41.8	74.6	19.7 ± 2.8	156.9 ± 4.2

J = 0.004530 ± 0.4 % total gas age: 147.3 ± 15.0
65 % plateau age: 154.5 ± 8.5

Tab.. 6: $^{40}Ar/^{39}Ar$ analytical data from fine-grained white mica, mylonite T-3, Tribeč Mts.

Step	T(C°)	% $^{39}Ar^*$	% $^{40}Ar^*$	$^{40}Ar/^{39}Ar$±2s. d.(%)	Age (Ma) ± 2s.d.
1	615	4.0	91.4	7.48 ± 1.1	62.8 ± 0.7
2	655	2.6	96.7	7.57 ± 1.8	63.6 ± 1.1
3	695	4.8	97.8	7.54 ± 0.7	63.3 ± 0.4
4	735	2.6	97.5	7.58 ± 1.5	63.7 ± 0.9
5	785	11.9	98.7	7.60 ± 0.5	63.8 ± 0.3
6	845	6.5	98.5	7.76 ± 0.5	65.2 ± 0.3
7	920	18.7	98.7	7.94 ± 0.3	66.6 ± 0.2
8	995	17.4	98.8	8.25 ± 0.3	69.2 ± 0.2
9	1050	21.4	98.9	8.49 ± 0.2	71.1 ± 0.1
10	1220	10.3	98.8	8.66 ± 0.5	72.6 ± 0.4

J = 0.004530 ± 0.4 % total gas age: 67.7 ± 0.6

Tab. 7: $^{40}Ar/^{39}Ar$ analytical data from medium-grained white mica, mylonite T-3, Tribeč Mts.,

Step	T(C°)	% $^{39}Ar^*$	% $^{40}Ar^*$	$^{40}Ar/^{39}Ar$±2s. d.(%)	Age (Ma) ± 2s.d.
1	620	3.3	74.4	8.09 ± 8.0	67.9 ± 5.3
2	690	6.2	88.6	8.96 ± 6.8	75.0 ± 5.0
3	790	10.5	91.7	8.67 ± 4.2	72.6 ± 3.0
4	920	47.4	96.7	8.51 ± 0.9	71.3 ± 0.6
5	1060	27.9	93.9	12.12 ± 1.2	100.8 ± 1.2
6	1350	4.8	67.0	31.02 ± 2.5	247.9 ± 5.9

J = 0.004530 ± 0.4 % total gas age: 88.3 ± 2.6
65 % plateau age71.4 ± 0.7

Tab. 8: $^{40}Ar/^{39}Ar$ analytical data from biotite, deformed granodiorite T-7, Tribeč Mts.

Step	T(C°)	% $^{39}Ar^*$	% $^{40}Ar^*$	$^{40}Ar/^{39}Ar$±2s. d.(%)	Age (Ma) ± 2s.d.
1	690	10.2	76.9	10.17 ± 2.0	88.2 ± 1.7
2	730	18.2	80.3	10.00 ± 1.4	86.7 ± 1.2
3	780	15.5	82.2	9.46 ± 1.2	82.1 ± 1.0
4	800	8.2	77.9	9.45 ± 2.4	82.0 ± 1.9
5	880	14.9	80.9	9.33 ± 1.7	81.1 ± 1.4
6	925	8.4	73.3	9.84 ± 2.8	85.4 ± 2.4
7	980	10.0	75.3	10.77 ± 2.1	93.2 ± 1.9
8	1080	9.7	77.0	12. 32 ± 2.4	106.3 ± 2.4
9	1250	4.8	65.5	12.82 ± 4.4	110.5 ± 4.7

J = 0.004530 ± 0.4 % total gas age: 88.5 ± 3.3

Tab. 9: $^{40}Ar/^{39}Ar$ analytical data from biotite, undeformed granodiorite, T-8, Tribeč Mts.

Step	T(C°)	% $^{39}Ar^*$	% $^{40}Ar^*$	$^{40}Ar/^{39}Ar$±2s. d.(%)	Age (Ma) ± 2s.d.
1	650	7.7	95.1	40.94 ± 1.1	332.2 ± 3.4
2	690	7.9	78.1	44.03 ± 2.0	355.1 ± 6.4
3	730	8.7	92.2	42.81 ± 0.9	346.1 ± 2.8
4	780	10.5	97.7	40.26 ± 0.6	327.1 ± 1.9
5	800	8.8	97.8	41.24 ± 1.0	334.5 ± 3.1
6	880	5.2	96.4	40.72 ± 1.8	330.6 ± 5.3
7	925	4.4	95.9	41.17 ± 1.0	333.9 ± 3.2
8	980	9.6	96.2	41.66 ± 1.2	337.6 ± 3.8
9	1080	23.5	97.9	41.17 ± 0.4	334.0 ± 1.1
10	1250	13.7	97.6	40.19 ± 0.8	326.6 ± 2.4

J = 0.004708 ± 0.4 % total gas age: 335.1 ± 4.9

Tab. 10: $^{40}Ar/^{39}Ar$ analytical data from biotite (biotite–albite enclave), undeformed granodiorite, T-9, Tribeč Mts.

Step	T(C°)	% $^{39}Ar^*$	% $^{40}Ar^*$	$^{40}Ar/^{39}Ar$±2s. d.(%)	Age (Ma) ± 2s.d.
1	650	22.1	98.0	47.11 ± 0.3	377.6 ± 1.1
2	690	22.5	98.1	46.35 ± 0.3	372.1 ± 1.1
3	730	4.4	96.5	48.31 ± 1.4	386.3 ± 5.0
4	780	4.4	96.6	49.59 ± 1.3	395.5 ± 4.7
5	800	22.3	97.9	49.12 ± 0.2	392.2 ± 0.7
6	880	7.4	97.7	48.70 ± 0.5	389.1 ± 1.9
7	925	13.9	97.8	46.49 ± 0.3	373.1 ± 1.2
8	980	1.1	96.7	46.63 ± 2.3	374.1 ± 7.6
9	1080	1.9	97.0	46.71 ± 2.5	374.7 ± 8.4

J = 0.004708 ± 0.4 % total gas age: 380.9 ± 3.4

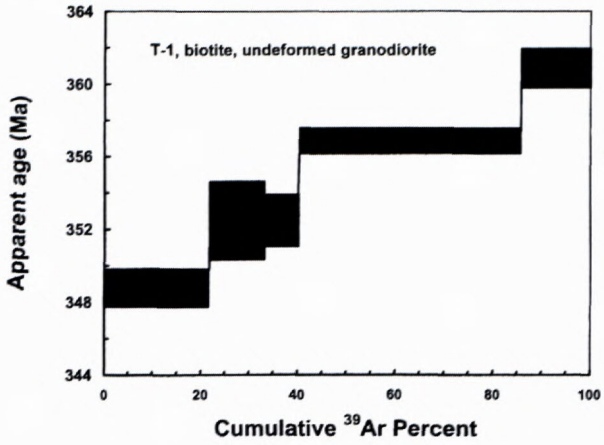

Fig. 9 $^{40}Ar / ^{39}Ar$ apparent age spectrum in sample T–1: Biotite from undeformed granodiorite.

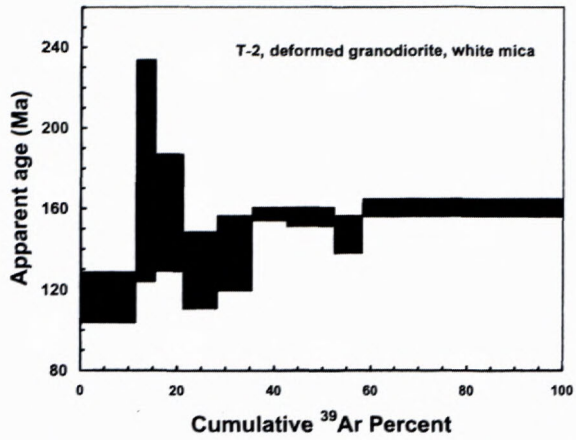

Fig. 10 $^{40}Ar / ^{39}Ar$ apparent age spectrum in sample T–2: medium-grained white mica from protomylonite.

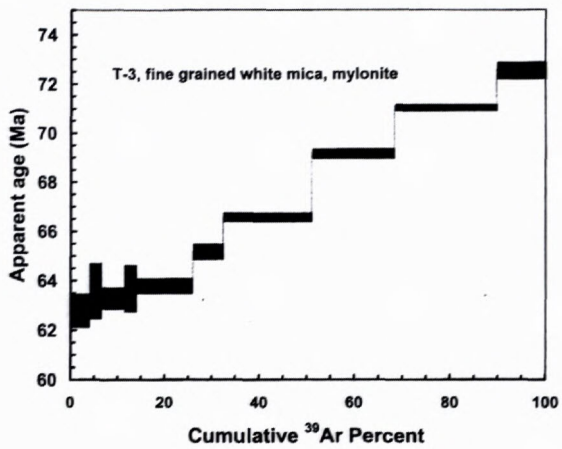

Fig. 11 $^{40}Ar / ^{39}Ar$ apparent age spectrum in sample T–3: fine-grained white mica from mylonite.

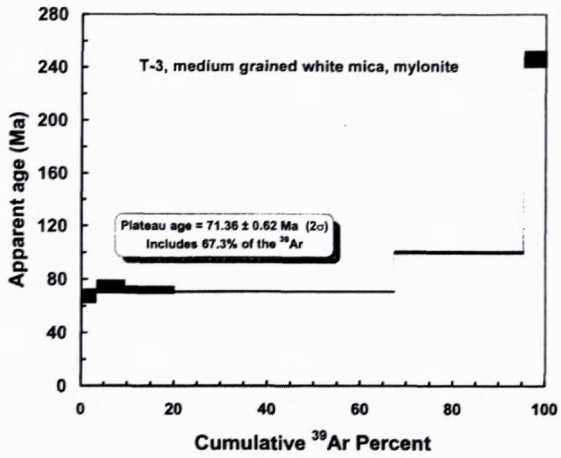

Fig. 12 $^{40}Ar / ^{39}Ar$ apparent age spectrum in sample T–3: medium-grained white mica from mylonite.

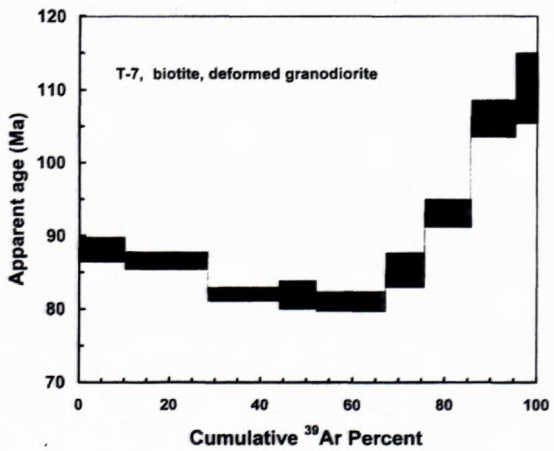

Fig. 13 $^{40}Ar / ^{39}Ar$ apparent age spectrum in sample T–7: biotite from deformed granodiorite

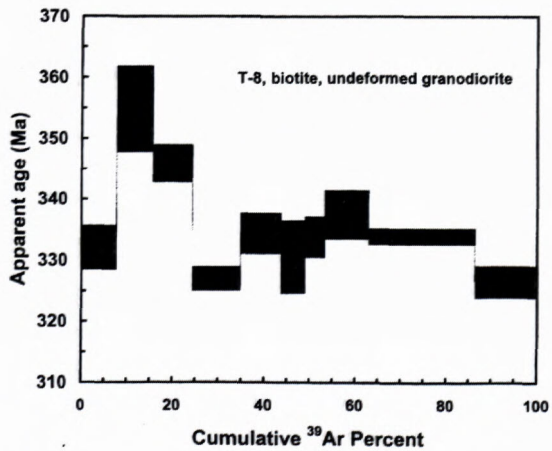

Fig. 14 $^{40}Ar / ^{39}Ar$ apparent age spectrum in sample T–8: biotite from undeformed granodiorite.

The variability of the shape of $^{40}Ar^*/^{39}Ar$ spectra, obtained from differently deformed granitoids of the Tribeč Mts., as well as the apparent ages alone have to be evaluated in this context. Though it is questionable whether obtained knowledge can be generalized for the whole Tribeč crystalline basement, the found results indicate that the relation of K/Ar system to the Alpine thermal and dynamic overprint on the rocks of this basement is definitely different in comparison with other core mountains with available primary data on their Hercynian cooling. The differences in the shape of $^{40}Ar^*/^{39}Ar$ mineral spectra, obtained from tectonically differently overprinted

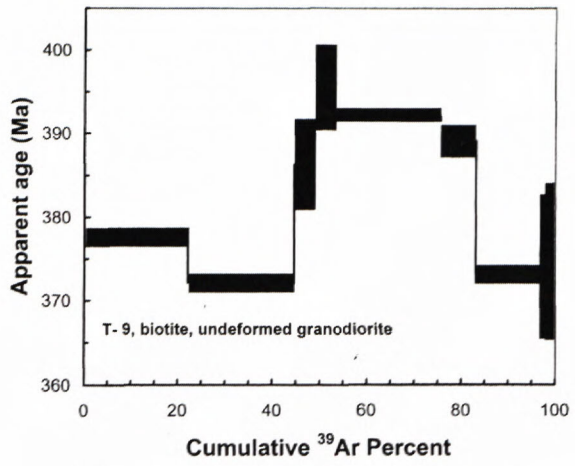

Fig. 15 ^{40}Ar / ^{39}Ar apparent age spectrum in sample T–9: biotite from albite–biotite enclave - undeformed granodiorite.

granitoid rocks of the Tribeč Mts. require wider analysis, preferably by control these data by Rb-Sr geochronometer.

From the sample T-3, representing typical mylonite, we have separated two kinds of white micas - medium-grained muscovite and fine-grained white mica (sericite). Light-coloured micas are the typical synkinematic minerals in rocks and can be used for dating of the mylonitization age (Figs. 4 and 5). The apparent $^{40}Ar^*/^{39}Ar$ muscovite ages of sample T-3 have a discordant character only in the higher-temperature part of the spectra. Apparent $^{40}Ar/^{39}Ar$ age 248 Ma in the last temperature step cannot be interpreted unambiguously, but the decisive volume of outgassed Ar from muscovite is represented by the plateau age 72 ± 2 Ma, that is within the analytical error coincident with the higher apparent age from sericite of the same sample. $^{40}Ar^*/^{39}Ar$ spectra of the apparent ages in sericite are of staircase shape proving for higher degassing temperature the apparent age ca 73 Ma and for the lowermost temperature of degassing 63 Ma. The staircase spectra of white micas from mylonitic zones are common and can be caused by the mixed mineral population of white mica different in age, next by the gradual diffusion lost of $^{40}Ar^*$ in the grains of different dimensions, and by the prolonged neocrystallization during formation of mylonite zones (Kirschner et al. 1996). Comparison of obtained spectra from quantitatively different mica types from this sample and their age concordance documents, that their age is tied with the age of origin of mylonite zone.

However, it is probable, that the anomalous biotite ages from undeformed rocks (T-1, T-8, T-9 - Figs. 9, 14, 15) are caused by excess argon in analysed biotite, which can be analytically separated from radiogenic argon, produced in biotite *in situ*, e.g. by different variants of isochron analysis of analytical data. As the reason of the excess argon in biotite there is supposed the high partial pressure of argon in the rock environment, that originates by degassing of rocks from the deeper crustal parts and which in certain tectonic circumstances (thrusting) penetrates their higher parts. This phenomenon was described in the crystalline basement of the Eastern Alps by Brewer (1969). For such argon entering into the structure of existing biotite, the temperature of environment must be higher as the blocking temperature of K-Ar system for biotite. Concerning the regional distribution of investigated samples, the argon excess in biotites from undeformed tonalites of Tribeč can be understood like characteristic phenomenon, spread at larger regional scale. It is not clear so far when the extraneous argon was captured by biotite. Because the excess argon is preserved mainly in undeformed granitoids, we suppose, that the excess origin can be joined with the deformation event and with the formation of mylonite zones.

The apparent ages spectra obtained from white fine-grained mica from the sample T-2 (Fig. 10) cannot be interpreted unequivocally. Though the Jurassic record is provable in $^{40}Ar^*/^{39}Ar$ spectra of apparent ages of various minerals also in other areas of crystalline basement of the Western Carpathians (Maluski et al. 1993, Kráľ et al. 1997, Hók et al. 2000), the process related to it is questionable. The white mica analysed in this sample is also secondary in origin. For formation of new sericite there is necessary the free potassium - it can be derived from the disintegration of biotite, but can be brought into rocks also by hydrothermal processes. By this way there were interpreted the Rb/Sr and $^{40}Ar^*/^{39}Ar$ Jurassic ages in the regions where the record about Alpine tectonothermal event is completely missing (e.g. Schwarzwald; Grauert et al. 1993, Lippolt and Kirsch, 1994). Potassium is deliberated during the chloritization of biotite and directly in this sample the biotite is strongly chloritized. Therefore we can suppose the temporal ties of origin of the newly-formed fine-grained mica in the sample T-2 with the strong chloritization of biotite.

The process of rock deformation in granitoids of the Tribeč Mts., being indicated by biotite from the sample T-7, had varying intensity. Presented spectra $^{40}Ar^*/^{39}Ar$ of apparent ages (Fig. 13) can be the demonstration of incomplete degassing of biotite during tectonic deformation in increased temperature, as is documented by minimum apparent ages from the medium-temperature part of the spectra.

Conclusion

The results of the examination of the shear zone in granitoid rocks in the north-western segment of the Zobor part of the Tribeč Mts. can be summarized as follows:

- granitoid rocks were affected by shear deformation having the character of progressive simple shear
- the strain rate of the rock was the highest in the centre of the shear zone and it corresponded to the value $\gamma = \mathbf{2.38}$
- compression during origin of the mylonite zone was oriented in N-S direction (the recent geographic orientation)
- physical and mechanical characteristics of granitoid rocks correlate with rock deformation, i.e. with the zonality of deformation
- $^{40}Ar/^{39}Ar$ ages obtained from the white micas from the centre of mylonite zones can be interpreted as the mylonitization ages

- the age of the origin of the shear zone suggests for the strong compression event, taking part at the boundary between Cretaceous and Paleogene
- the accepting of the age of tonalite intrusion 306 ± 10 Ma as well as knowledge on the crystalline basement cooling in other Core Mountains indicate, that granitoid rocks in the Tribeč Mts. were exposed to higher temperatures than the blocking temperatures in K-Ar systems in biotites. It is confirmed by excess argon in biotites from undeformed granitoid rocks, but also by the loss of radiogenic Ar from biotites of partly deformed rocks. The age of this process is not clear up till now, but we can assume, that it is related to the distinct tectonothermal event, that caused deformation and decisive metamorphic overprint in rocks of cover sequence (Lower Triassic-Lower Cretaceous, Ivanička et al. 1998), resp. mylonitization (ca 70 Ma). From this viewpoint the Tribeč Mts., as a core mountain is exceptional, because such demonstrations in the majority of Core Mountains were not documented yet in such a range.

Appendix

Location of sampling sites

T-1, undeformed granodiorite, Veľké Jastrabie Valley, ca 1300 m to SW from the holiday resort Koželužne Bošany.

T-2, partly mylonitized granodiorite, Veľké Jastrabie Valley, identical locality as T-1

T-3, central part of mylonitized zone, Veľké Jastrabie Valley, identical locality as T-1

T-7, mylonitized granodiorite, mountain ridge, 1000 m to SSW from the altitude point Medvedí (719.4 m above sea level), Tribeč Mts.

T-8, granodiorite, the Žľaby locality (520 m above sea level), ca 700 m to SSW from the altitude point Javorový vrch (730 m above sea level), rock outcrop, Tribeč Mts.

T-9, mafic enclave in granodiorite, rock outcrop, identical locality as T-8, Tribeč Mts.

References

Bagdasaryan, G.P., Cambel B. & Veselský, J. 1977: Potassium age determination of rocks of crystalline complexes from the West Carpathians and their preliminary interpretation (in Russian). *Geol. Zbor. , Geol. carpath., 28, 2, 219 –242.*

Bagdasaryan, G.P., Gukasyan, R., Kh., Cambel, B., Broska, I. 1990: Rb-Sr isochrone dating of granitoids from Tribeč Mts. Geologický zborník, Geologica Carpath., 41,4, 437-442.

Berthé, D., Choukroune, P. & Jegouzo, P. 1979: Orthogneiss, mylonite and non-coaxial deformation of granite: the example of the South Armorican shear zone. Journal of Structural Geology, 1, 31 - 42.

Bieniawski, Z.T., 1973: Engineering classification of jointed rock masses. Transact. S. Afr. Ins. Civil Eng., 15, p. 335-342.

Bojko, A.K., Kamenický, L., Semenenko, N.P., Cambel, B. & Shcherbak, N.P. 1974: Part of results of dating of absolute ages of rocks from crystalline massif of the Western Carpathians and the recent state of knowledge. *Geologický zborník, Geologica Carpath., 1, 25, 25 - 39.* (In Russian)

Brewer, M. S. 1969: Excess radiogenic argon in metamorphic micas from the Eastern Alps. *Earth Planet. Sci. Lett., 6, 321 – 331.*

Broska, I & Petrík, I. 1993: Tonalite of Sihla type sensu lato: Variscan plagioclase-biotite magmatite of I -type in Western Carpathins. Mineralia Slovaca, 25, 23 - 28. (in Slovak)

Broska, I., Bibikova, E.V., Gracheva, T.V., Makarov, V.A. & Caňo, F. 1990: Zircon from granitoid rocks of the Tribeč-Zobor crystalline complex: its typology, chemical and isotopic composition. *Geologický zborník, Geologica Carpath. 41, 4, 395 - 416.*

Burchart, J., Cambel, B., Kráľ, J. 1987: Isochron reassessment of K-Ar dating from the Western Carpathian crystalline complex. Geol. Zborn., Geol. Carpath., 38, 2, 131 – 170.

Fediuk, F. 1961 : Fiodorov microscopic method. Publishing house ČSAV, Praha. (In Czech)

Grauert, B., O´Brien, P. J. & Lork, A. 1993: Rb-Sr dating of Jurassic low-temperature potassium metasomatism in gneisses of the Schwarzwald, Germany. Abstract suppl. 1 to Terra Nova 5, p. 386.

Hók J., Siman P., Frank, W. Kráľ, J., Kotulová J. & Rakús, M. 2000: Origin and exhumation of mylonites in Lúčanská Malá Fatra Mts., the Western Carpathians. *Slovak Geol. Mag. 6,4, 325 – 334.*

Ivanička, J., Hók, J., Polák, M., Határ, J., Vozár, J., Nagy, A., Fordinál, K., Pristaš, J., Konečný, V., Šimon, L., Kováčik, M., Vozárová, A., Fejdiová, O., Marcin, D., Liščák, P., Macko, A., Lanc, J., Šantavý, J. & Szalaiová, V. 1998: Explanations to geological map of Tribeč Mts. 1 : 50 000. Geological Survey of Slovak Republic, Dionýz Štúr Publishers, Bratislava, 7 - 237.

Jánová, V., 1997: Monitoring of dynamics of weathering processes development in semi-rock environment. Proceedings from 3rd geotechnical conference. STU - Bratislava. (in Slovak)

Jánová, V., Liščák P., 1998: Monitoring of weathering processes. Supplement No. 3 to Partial monitoring system of geological factors of living environment of Slovak Republic. GS SR Bratislava. (in Slovak)

Kirschner, D. L., Cosca, M. A., Masson H. & Hunziker, J. C. 1996: Staircase $^{40}Ar/^{39}Ar$ spectra of fine grained white mica: Timing and duration of deformation and empirical constraints on argon diffusion. *Geology, 24, 8, 747–750.*

Kohút, M. Kráľ, J., Michalko, J. & Wiegerová V., 1998: Hercynian cooling of the Veľká Fatra massif – evidences from $^{40}K/^{40}Ar$ and $^{40}Ar/^{39}Ar$ thermochronometrical mineral data and the recent state of thermochronometry. *Mineralia Slovaca, 30, 253–264.* (in Slovak)

Kohút, M., Todt, W., Janák, M. & Poller, U. 1999: Rapid exhumation of the Variscan basement in the Veľká Fatra Mts. (Western Carpathians – Slovakia). In: *Alpine evolution of the Western Carpathians and related areas (eds. Plašienka D., Hók J., Vozár, J., Elečko M.). Geological Survey of Slovak republic, 21 – 22.*

Kováč, M., Kráľ, J., Márton, E., Plašienka, D. & Uher, P. 1994: Alpine uplift history of the central Western Carpathians: geochronological, paleomagnetic, sedimentary and structural data. *Geologica Carpathica, 45, 2, 83 - 96.*

Kráľ, J., Hess, J., C., Kober, B. & Lippolt, H., J. 1997: $^{207}Pb/^{206}Pb$ and $^{40}Ar/^{39}Ar$ age data from plutonic rocks of the Strážovské vrchy Mts basement, Western Carpathians. In: *Geological evolution of the Western Carpathians (Grecula, P., Hovorka, D. & Putiš, M. (eds.). Mineralia slov. - Monograph, Bratislava, 253 - 260.*

Lippolt, H., J. & Kirsch, H. 1994: Isotopic investigation of Post/Variscan plagioclase sericitization in the Schwarzwald Gneiss Massif. Chem. Erde, 54, 179 - 198.

Lister, G.S. & Williams, P.F. 1979: Fabric development in shear zones: theoretical controls and observed phenomena. Journal of Structural Geology, 1, 283 - 297.

Maluski, H., Rajlich, P. & Matte, P. 1993: ^{40}Ar-^{39}Ar dating of the Inner Carpathians Variscan basement and Alpine mylonitic overprinting. *Tectonophysics, 223, 319 - 337.*

McDougal, I. & Harrison, T. M. 1988: Geochronology and thermochronology by the $^{40}Ar/^{39}Ar$ method. Oxford University Press, New York, 212 p.

Petrík, I., Broska, I. & Uher, P. 1994: Evolution of the Western Carpathian granite magmatism: age, source rocks, geotectonic setting and relation to the Variscan structure. Geologica Carpathica, 45, 5, 283 - 291.

Ramsay, J.G. 1980: Shear zone geometry: a review. Journal of Structural Geology, 2, 1/2, 83 - 99.

Shcherbak, N. P., Bartnitsky, E. N., Mitskievitch, N. Y., Stepanyuk, L. M., Cambel, B. & Grecula, P. 1988: U-Pb radiometric determination of the age of zircons from Modra granodiorite (Malé Karpaty) and porphyroid from Spišsko–gemerské rudohorie Lower Paleozoic, (Western Carpathians). In Russian. *Geol. Zbor. , Geol. carpath., 39, 4, 427 – 436.*

Shcherbak, N., P., Cambel, B., Bartnitsky, E., N. & Stepanyuk, L., M. 1990: U-Pb age of granitoid rock from the quarry Dubná Skala - Malá Fatra Mts. *Geol. Zborn., Geologica Carpathica, 41, 4, 407-414.*

Shelley, D. 1993: Igneous and metamorphic rocks under the microscope. *Chapman and Hall, London, 445 p.*

Sibson, R. H. 1980: Transient discontinuities in ductile shear zones. Journal of Structural Geology, 2, 1/2, 165 – 171.

Sibson, R., H. 1977: Fault rocks and fault mechanism. Journal of the Geological Society of London, 133, 190 - 213.

Steiger, R.H. & Jäger, E. 1977: Subcommision on geochronology: convention on the use of decay constant in geo- and cosmochronology. *Earth Planet. Sci. Lett. , 36, 359 – 362.*

STN 73 1001: Foundation soil beneath areal foundations

Vass, D., Began, A., Gross, P., Kahan, Š., Köhler, Lexa, J. a Nemčok, J. 1988: Regional geological division of the Western Carpathians and northern promontory of Pannonian basin in the area of CSSR. 1 : 500 000. SGÚ - GÚDŠ, Bratislava.